A gas bubble-based parallel micro manipulator: conceptual design and kinematics model

Wei Dong[1,3], Michael Gauthier[1], Cyrille Lenders[2] and Pierre Lambert[1,2]

[1] Department of Automatic Control and Micro-Mechatronics Systems, FEMTO-ST Institute, CNRS UMR 6174-UFC/ENSMM/UTBM, 24, Rue Alain Savary, 25000 Besancon, France
[2] Bio Electro and Mechanical Systems Department, Université libre de Bruxelles (U.L.B), Av. F.D. Roosevelt 50, 1050 Bruxelles, Belgium
[3] State Key Laboratory of Robotics and System, Harbin Institute of Technology, Post Box 3005, 2 Yikuang Street, Harbin 150080, China

Abstract

The parallel mechanism has become an alternative solution when micro manipulators are demanded in the fields of micro manipulation and micro assembly. In this paper, a three-Degree-Of-Freedom (3-DOF) parallel micro manipulator is presented, which is directly driven by three micro gas bubbles. Since the micro gas bubbles are generated and maintained due to the surface tension between the gas and liquid media, the proposed novel system can be used in the liquid environment which allows for rotation about *X* and *Y* axis and translation in *Z* axis. In this paper, the conceptual design of micro gas bubble-based parallel manipulator is introduced and the input/output characteristic of the actuator is analyzed in detail. The kinematics model of the parallel micro manipulator is also established, based on which the workspace and the system motion resolution are analyzed as a criteria and reference for future prototype development.

1. Introduction

Micro-actuators and micro-sensors are currently mainly based on smart materials which are typically able to induce movement based on electric field (e.g. piezoelectricity [1-3]), on magnetic field (e.g. magnetic shape memory alloy [4]) or temperature control (e.g. thermal shape memory alloy [5-6]). Recently a new kind of actuators called *fluidic flexible actuators* has been proposed in the centimeter scale [7-9]. They are based on the transduction between a hydraulic or pneumatic energy *P.V* into a mechanical energy *F.d* through a flexible membrane. The hydraulic or pneumatic energy easily delocalizes the control parameters (*P, V*) far away from the transducer. This advantage seems to be relevant in the micro-scale where space is usually highly limited. However, downsizing of these actuators is limited by the miniaturization of the membrane confining the gas or liquid. This paper is proposing a study on a micro-robot based on a new transducer between pneumatic energy and mechanical energy where the membrane is simply obtained using the capillary interface between the gas and a liquid [10, 11]. This *capillary actuator* is only relevant when the typical dimension is lower than the capillary length which represents the length making the cut-off between gravity effects and surface tension effects. This novel system is driven by equilibrium between the compressibility of the gas and the capillary pressure induced by the curvature of the interface and therefore has some original properties in term of actuation and sensing [10]. Moreover the intrinsic and controllable compliance of the bubbles is a particularly interesting property in order to compensate positioning errors in the packaging of fragile micro-systems. The relevance of this actuation principle has been proved in practice and the concept of micro bubble based parallel manipulator, i.e. several gas bubbles drive a common end-platform, also

has been validated in the previous works [11-12] as shown in Figure 1. This paper deals with the performances of parallel micro-robots based on three capillary actuators.

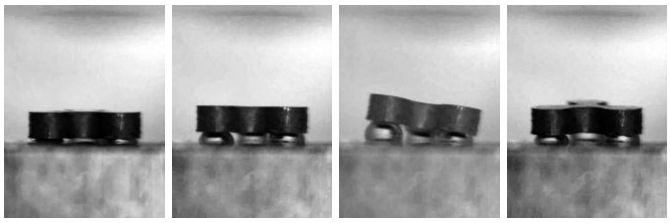

(a) (b) (c) (d)

Figure 1. Lateral view of an example of parallel robot based on capillary actuation. Three bubbles are used to actuate the micro-robot: (a) initial position; (b) vertical displacement; (c and d) rotational displacement

Parallel type micro-robot is a usual way to obtain multi-Degree-Of-Freedom with a good repeatability. High precision parallel robot is marginally based on conventional universal joints [13] and usually based on compliant joints [15-21], and marginally on active joints based, for example, on SMA actuation [14]. In order to realize large workspace and high precision simultaneity, dual actuation technique is also utilized in the parallel mechanisms, in which two precision level actuators, for example, conventional motors and piezoelectric stacks work as coarse and fine actuators respectively [22-24].

In the micro-scale, capillary forces are significant and they have been used to induce micromanipulation or micro-actuation. In micro-fluidic, bubbles are currently used in several ways: (i) acoustic oscillating bubbles enables controlled fluid flow around the bubble [25-28], (ii) bubbles are used as actuator moving a mechanical compliant system [29] or closing a micro-channel [30], (iii) bubbles are used as a compliant kinematical link actuated by an external force [31-33]. In the case of capillary actuated robot proposed in this paper, the capillary cap represents the actuator and also the kinematic joint. This originality enables to design a very compact structure but the modeling of the robotic structure is becoming more complex.

This paper is proposing an analysis of this original robot. Firstly the conceptual design of the parallel micro manipulator is proposed. The micro gas bubble behavior which is the elementary actuator in the system is presented. Based on this, the kinematics analysis to produce the input-output relationship between the actuators and the end-platform is also presented which is necessary for positioning applications, and finally the workspace of the system is analyzed as performance evaluation for the future design of the prototype.

2. Conceptual design

A schematic diagram of the proposed parallel micro manipulator is illustrated in Figure 2. As it can be observed that the conceptual design of the parallel micro manipulator consists of a top movable plate called the end-platform, a bottom fixed plate called the substrate (static base), and three micro gas bubbles between the end-platform and the substrate, with the viewpoint of mechanism analysis, it can be considered as a three legs parallel micro manipulator system.

It can be seen that there are three fabricated through holes in the end-platform which can be called contact holes. The end-platform can be supported and maintained by the micro gas bubbles via these three contact holes. The micro gas bubbles are confined by the gas-liquid interface because of the surface tension between the two media. In fact, the contact between the end-platform and micro gas bubbles can be self-aligned due to the interaction force between the interfaces. The volume of the gas bubbles can be compressed or

decompressed when the pistons move along the inlet tubes which are drilled into the substrate. Therefore, if the three pistons are commanded simultaneously, the position and pose of the end-platform of the parallel manipulator can be controlled. With the viewpoint of robotics, the parallel micro manipulator system proposed in this design can provide 3-DOF motion, rotation about *X* and *Y* axis and translation along *Z* axis.

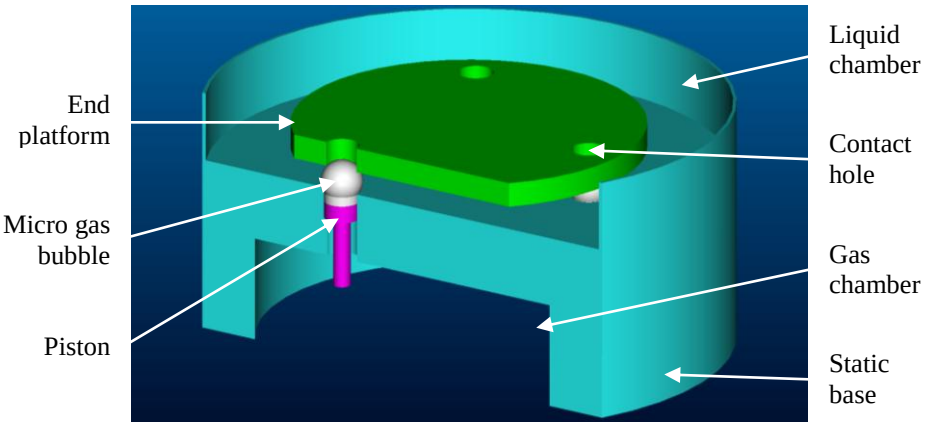

Figure 2. The 3D model of the proposed parallel micro manipulator base on the micro gas bubbles

3. Actuator characterization

The performance of the parallel micro manipulator depends on the characteristic of the actuators, so it is necessary to discuss the characteristic of the micro gas bubble before establishing the kinematics model of the integrated system. From the conceptual design of the system (Figure 2) and the sketch of the micro gas bubble (Figure 3), it can be seen that position and pose of the parallel micro manipulator system is directly related with the gap (variable ***h***) between the end-platform and the substrate. The variable ***h*** is ultimately controlled by the variable ***u*** which is the distance between the substrate surface and the piston surface (the arrows of ***h*** and ***u*** in Figure 3 indicate the positive directions). When the piston moves along the vertical axis, the volume of the micro gas bubble will be compressed or decompressed which correspondingly controls the value of variable ***h***.

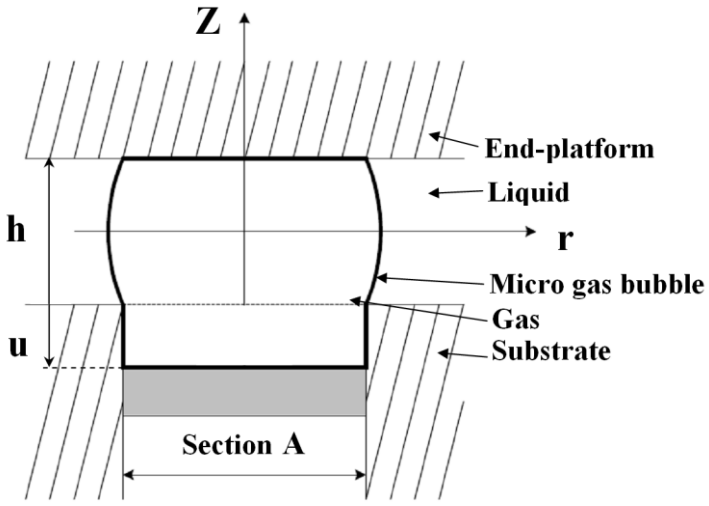

Figure 3. Sketch of a single micro gas bubble actuator

Since the micro gas bubble is a typical flexible actuator which will be deformed when an external load is applied, the behaviors of the micro gas bubbles should be discussed individually. The generic model of gas bubble is firstly ruled by two basic physics laws,

Young-Laplace Equation and Ideal Gas Law [34]. If the pressure gap between both sides of the meniscus interface is ***dp***, it can be formulated as below based on Young-Laplace Equation,

$$dp = 2H\gamma \tag{1}$$

where 2***H*** is the curvature of the meniscus and ***γ*** is the surface tension.

The pressure inside the meniscus ***p*** can be expressed according to Ideal Gas Law

$$pV = (p_0 + dp)\cdot(V_{cap} + uA) = nRT \tag{2}$$

where ***V*** is the total volume, $\boldsymbol{p}_0$ is the pressure outside the meniscus, $\boldsymbol{V}_{\text{cap}}$ is the volume inside the meniscus, ***n*** is the amount of substance, ***R*** is the gas constant, ***T*** is the absolute temperature, and as mentioned above, ***u*** is the piston position and ***A*** is the section of the piston.

It can be assumed that the meniscus profile can be formulated as a parabola,

$$r(z) = a_0 + a_2 z^2 \tag{3}$$

where $\boldsymbol{a}_0$ and $\boldsymbol{a}_2$ are the parameters to be determined, the definition of ***r*** and ***z*** can be referenced to Figure 3. For the applications involved in this paper, it is hypothesized that the bubble's meniscus profile is always maintained during the end-platform's motion.

Based on the geometrical condition that the parabola passes through the edges of the substrate, the formulation below can be written.

$$r = a_0 + \frac{a_2 h^2}{4} \tag{4}$$

On the other hand, the curvature 2***H*** can be expressed based on $\boldsymbol{a}_0$ and $\boldsymbol{a}_2$.

$$2H = -2a_2 + \frac{1}{a_0} \tag{5}$$

In addition, the capillary force ***f*** can be formulated as below,

$$f = -2a_2\gamma\pi a_0^2 - \pi\gamma a_0 \tag{6}$$

The volume in the meniscus $\boldsymbol{V}_{\text{cap}}$ can be obtained based on the profile of the meniscus.

$$V_{cap} = \pi\int_{-h/2}^{h/2} r^2(z)dz = \pi\left(\frac{a_2^2 h^5}{80} + \frac{a_0 a_2 h^3}{6} + a_0^2 h\right) \tag{7}$$

Combining the equations (1) to (7), the numerical model of the micro gas bubble can be obtained. In order to clearly indicate new actuator's performance, a numerical simulation is performed based on the model above.

Figure 4 shows the relationship between the variable ***u*** and variable ***h*** when the external force changes from 100 μN to 1600 μN with double increase. The overview of the curves indicates that the micro gas bubble actuator is a potential micro-actuator with high resolution, since it can be seen that the output varies from 0 to 500μm when input varies approximately from 1 to 10 mm. The ratio of output to input is about 1/20, which means the micro gas bubble will be high resolution actuator if the input can be controlled precisely.

From Figure 4 (a), it also can be seen that the relationship between output ***h*** and input ***u*** shows nonlinear behavior. Especially, a relatively larger external force will induce that the nonlinear phenomenon is more intensive (e.g. the purple curve F=1600μN in Figure 4 (a)). On the contrary, a small external force makes the input/output close to a linear system (e.g. the blue curve F=100μN in Figure 4 (a)). That phenomenon can be explained by the fact that a large external force induces large gas compress. That characteristic can be considered as a

saturation behavior of the micro gas bubble output when the piston is close to the substrate edges.

In Figure 4(b) a zoomed window of Figure 4(a), it also can be found that at the initial range of the actuation, the output ***h*** and input ***u*** shows a strict linear relationship, and in addition, the curves are parallel to each other when different external loads are applied on the bubble. The influence from difference external forces embodies different initialized position since a large external force means more volume of the gas bubble is compressed, and consequently a lower position will be obtained. On the other hand, when the external force is fixed, for each curve, the proportion of output ***h*** and input ***u*** is a constant ***k***. It means micro gas bubble as an actuator can be considered as a constant proportion link between output and input, in which the initial value can be determined when the value of external load is specified. The model of the micro gas bubble as an actuator can be formulated as $h = k \cdot u + h_{in}$ where $\boldsymbol{h_{in}}$ is the initialized value of ***h*** when the specified force is applied. This approximate linear model only can be used in the range of initial actuation (e.g. the range of input ***u*** from 7mm to 9.5 mm in Figure 4(a)), while the control model suitable to the full range has to yield to the nonlinear model.

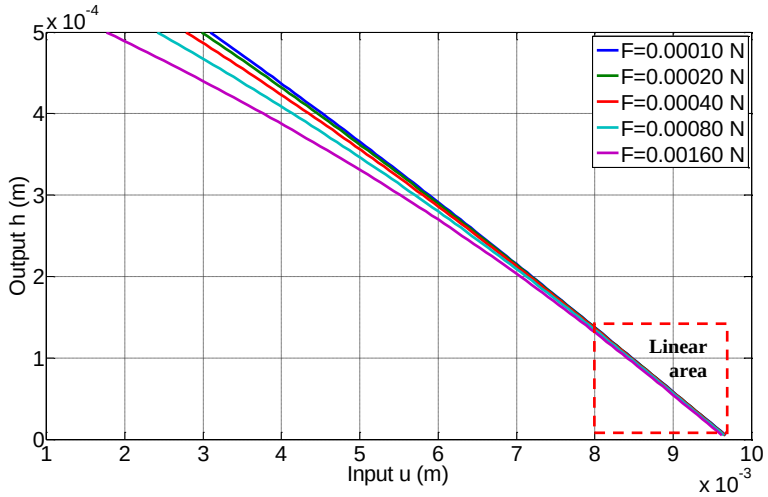

(a) Nonlinear behavior of the micro gas bubble actuation in the full range

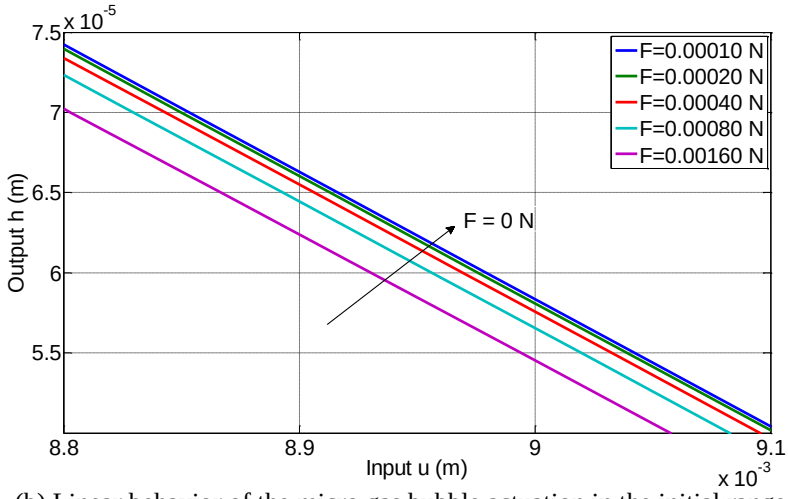

(b) Linear behavior of the micro gas bubble actuation in the initial range

Figure 4. The characterization of the micro gas bubble actuator

4. Kinematics model and Workspace Analysis

The kinematics modeling is always necessary for a parallel-type manipulator in the actual applications, which is needed for the real-time control of the prototype in the implementation. Especially for a flexible components (micro gas bubbles) involved parallel manipulator system, almost all of the performances analysis depends on a correct and reliable kinematics model, which will be discussed in detail in this section.

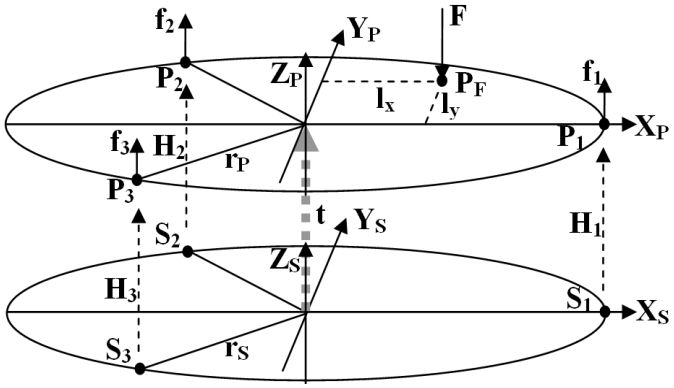

Figure 5. Kinematics model of the proposed parallel micro manipulator

In order to investigate the kinematics model of the proposed manipulator, two coordinate frames are assigned, as shown in Figure 5. A static Cartesian coordinate frame $\mathbf{X_S Y_S Z_S}$ is fixed at the center of the substrate while a mobile Cartesian coordinate frame $\mathbf{X_P Y_P Z_P}$ is assigned to the center of the mobile platform. $\mathbf{P_i}$ and $\mathbf{S_i}$ (i=1, 2 and3) are center points that are located in the holes center of the platform and the piston tube center of the substrate, respectively. Let $\mathbf{r_S}$ and $\mathbf{r_P}$ be the radii of the substrate and the platform passing though joints $\mathbf{P_i}$ and $\mathbf{S_i}$ (i=1, 2 and 3), respectively. It is convenient for a generic discussion that the radii are recorded as $\mathbf{r_S}$ and $\mathbf{r_P}$, although they equal to each other in our applications. The position of $\mathbf{S_i}$ with reference to the fixed coordinate frame $\mathbf{X_S Y_S Z_S}$ can be written as below in equation (8).

$$\begin{aligned} S_1 &= \begin{bmatrix} r_S & 0 & 0 \end{bmatrix}^T \\ S_2 &= \begin{bmatrix} -\frac{1}{2} r_S & \frac{\sqrt{3}}{2} r_S & 0 \end{bmatrix}^T \\ S_3 &= \begin{bmatrix} -\frac{1}{2} r_S & -\frac{\sqrt{3}}{2} r_S & 0 \end{bmatrix}^T \end{aligned} \tag{8}$$

The position of $\mathbf{P_i}$ can be expressed with respect to the mobile platform frame $\mathbf{X_P Y_P Z_P}$ as below in (9)

$$\begin{aligned} P_1 &= \begin{bmatrix} r_P & 0 & 0 \end{bmatrix}^T \\ P_2 &= \begin{bmatrix} -\frac{1}{2} r_P & \frac{\sqrt{3}}{2} r_P & 0 \end{bmatrix}^T \\ P_3 &= \begin{bmatrix} -\frac{1}{2} r_P & -\frac{\sqrt{3}}{2} r_P & 0 \end{bmatrix}^T \end{aligned} \tag{9}$$

So the kinematics model can be expressed as below in (10)

$$\vec{t} + R \cdot \vec{P}_i = \vec{H}_i + \vec{S}_i \tag{10}$$

where $\vec{t}$ is the translation vector of the end platform center with respect to the substrate frame $\mathbf{X_S Y_S Z_S}$. According to the kinematics of the proposed parallel micro manipulator, the

translational DOF of the system is translation of the mobile system with respect to *Z* axis, so the vector $\vec{t}$ can be expressed as the displacement of the end platform along the vertical *Z* axis.

$$t = \begin{bmatrix} 0 & 0 & Z \end{bmatrix}^T \tag{11}$$

R is the orientation matrix of the end platform with respect to the substrate frame $\mathbf{X_S Y_S Z_S}$. The end platform only can output two-axis rotation motion, so the matrix ***R*** can be formulated as the orientation (***α*** and ***β***) of the end platform about ***X*** and ***Y*** axis.

$$R = A_Y \cdot A_X = \begin{bmatrix} \cos\beta & 0 & \sin\beta \\ 0 & 1 & 0 \\ -\sin\beta & 0 & \cos\beta \end{bmatrix} \cdot \begin{bmatrix} 1 & 0 & 0 \\ 0 & \cos\alpha & -\sin\alpha \\ 0 & \sin\alpha & \cos\alpha \end{bmatrix} = \begin{bmatrix} \cos\beta & \sin\alpha\cdot\sin\beta & \cos\alpha\cdot\sin\beta \\ 0 & \cos\alpha & -\sin\alpha \\ -\sin\beta & \cos\beta\cdot\sin\alpha & \cos\alpha\cdot\cos\beta \end{bmatrix} \tag{12}$$

$\mathbf{H_i}$ is the vector between the holes center of the platform and the piston tube center of the substrate. Since the rotation angle (***α*** and ***β***) of the proposed system is limited to several degrees, the first two components of $\mathbf{H_i}$ can be considered as zero. In addition, combined with the discussion of Section 3, the vector $\mathbf{H_i}$ can be expressed as the gap distance between the platform and substrate $\mathbf{h_i}$.

$$H_i = \begin{bmatrix} 0 & 0 & h_i \end{bmatrix}^T \tag{13}$$

Differing with the pure rigid mechanisms, the force constraint has to be considered in the kinematics model of flexible components involved designs. In Figure 5, a normal force ***F*** is applied on the end platform with the contact point $\mathbf{P_F}$ whose distances to the **X** and **Y** axis are $\mathbf{l_x}$ and $\mathbf{l_y}$ respectively. So the force constraint can be expressed as below

$$\begin{aligned} \sum F_Z &= F + f_1 + f_2 + f_3 = 0 \\ \sum M_X &= f_1 \cdot l_{1Y} + f_2 \cdot l_{2Y} + f_3 \cdot l_{3Y} + F \cdot l_y = 0 \\ \sum M_Y &= f_1 \cdot l_{1X} + f_2 \cdot l_{2X} + f_3 \cdot l_{3X} + F \cdot l_x = 0 \end{aligned} \tag{14}$$

where $\boldsymbol{f}_1$, $\boldsymbol{f}_2$ and $\boldsymbol{f}_3$ are the actuation forces from three micro gas bubbles respectively, and $\boldsymbol{l}_{ij}$ (i=1, 2, or 3, and j=*X* or *Y*) is the *X* or *Y* axis component value of the vector from $\mathbf{P_i}$ to the point $\mathbf{P_F}$ (shown in Figure 5).

Combining the equations from (1) to (14), the kinematics model of the proposed parallel manipulator can be formulated, which can be used in the performances analysis for the proposed manipulator design and the real-time control for the fabricated prototype in the future.

As a parallel micro manipulator, the reachable workspace is a basic and important index through which the motion capability of the proposed system can be evaluated. As an example, a manipulator where $\mathbf{r_S}$=$\mathbf{r_P}$=10.0mm, $\mathbf{u_1}$, $\mathbf{u_2}$ and $\mathbf{u_3} \in$ [1 mm, 9.5 mm], a vertical force with 1500μN applied on the center point of the end platform, is considered to present the motion capability.

Figure 6 shows the workspace of the proposed parallel micro manipulator system when the rotation motion is required simultaneously. The maximum and minimum positions along the Z direction are 490 μm and 20 μm respectively (total motion range is 470 μm), when the full range of the actuation is reached (1 - 9.5 mm). The rotation motion capability is ±1.5 degrees and ±1.8 degrees in *X* axis and *Y* axis, respectively. From Figure 6, it also can be seen that the rotation motion has a significant impact on the Z motion stroke, i.e. motion capability of the parallel system along Z axis is sharply decreased when a relatively larger rotation motion is requested. It can be read from Figure 6, e.g. the motion range along *Z* axis is sharply reduced to 70 μm from 470 μm when the rotation angles about *X* axis (-1^o) and *Y* axis (1^o) are simultaneously provided by the proposed parallel manipulator.

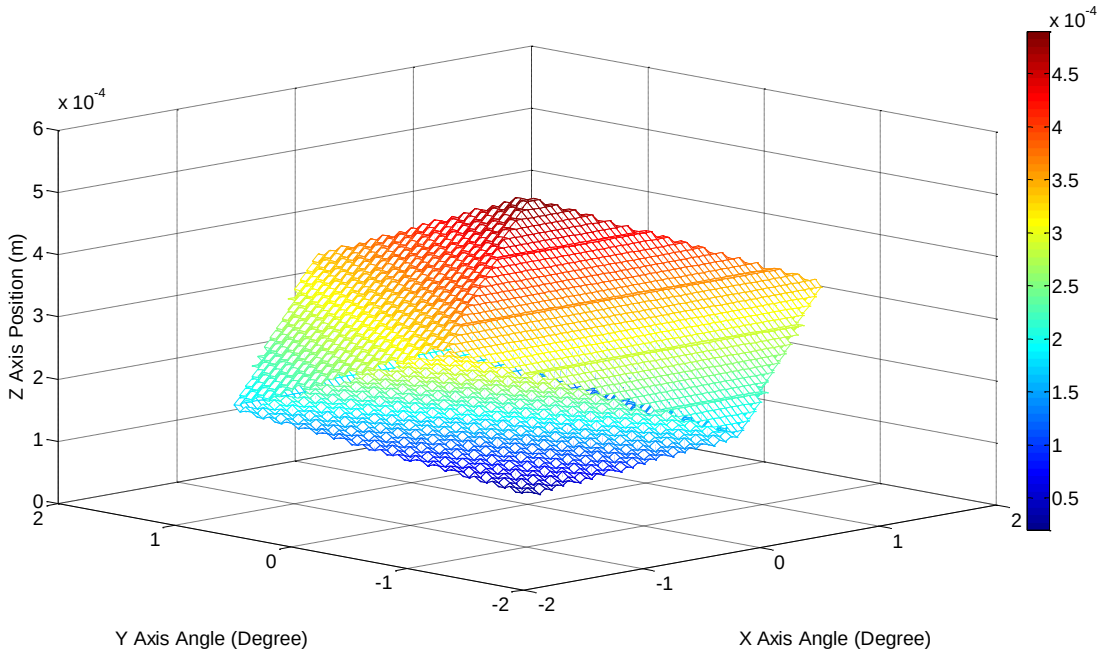

Figure 6. The Z direction motion capability of the proposed parallel micro manipulator

As mentioned in the previous section, micro gas bubble is a high resolution actuator since the displacement value of bubble output is much lower than the displacement value of piston input. A micro gas bubble embedded parallel manipulator also shows the characteristic of high resolution, which can be seen from aforementioned analysis (piston input is on mm level and the end-platform output is on μm level shown in Figure 6). A detailed quantitative analysis of system resolution is also presented in Figure 7, in which the analysis is performed under the same condition. The resolution of the piston input is assumed as 30 nm which is easy to be realized on actual implementation (e.g. piezoelectric stack actuator based dual actuation system which can guarantee high precision and wide motion range simultaneously). The resolution of the end-platform in Z direction is analyzed on different position level. From Figure 7, it can be seen that overall level of the end-platform resolution is about 2 nm if the input resolution is set to 30 nm, which indicates the proposed parallel manipulator is a high resolution system. In addition, the nonlinear behavior of the actuator also induces exclusive features of the parallel manipulator system. The average resolution is increased as the position of the end-platform is increased, which can be seen from Figure 7 (a)-(c). Figure 4 shows that the actuator indicates a high resolution performance in the nonlinear area. Comparing Figure 7 (a)-(c), a high position of the end-platform leads the pistons to work in the nonlinear area, so the average resolution is higher when the end-platform moves within high position level. From Figure 7 (a)-(c), it also can be seen that the resolution is variable even on the same position level, i.e. the resolution distribution is a curved surface but not a planar one which shows the resolution on the margin is relatively higher and the one on the center is low. Margin points on the surface mean that end-platform works with a large pose. That can be understood that the micro gas bubble is approaching to the stoke limit, i.e. working in the nonlinear area, so the system's resolution is relatively higher. Moreover, the nonlinear features of the actuation leads to that the resolution distribution surfaces for different Z locations are not parallel to each other along the Z direction. The application of micro gas bubbles induces the parallel manipulator system to reflect exclusive characteristics, e.g. high motion resolution, which is significant for micro-manipulation and micro-assembly in liquid environment. If the resolution is critical for the applications in the full workspace of the system, it should be dealt with sensitively during the system design and dimensional synthesis.

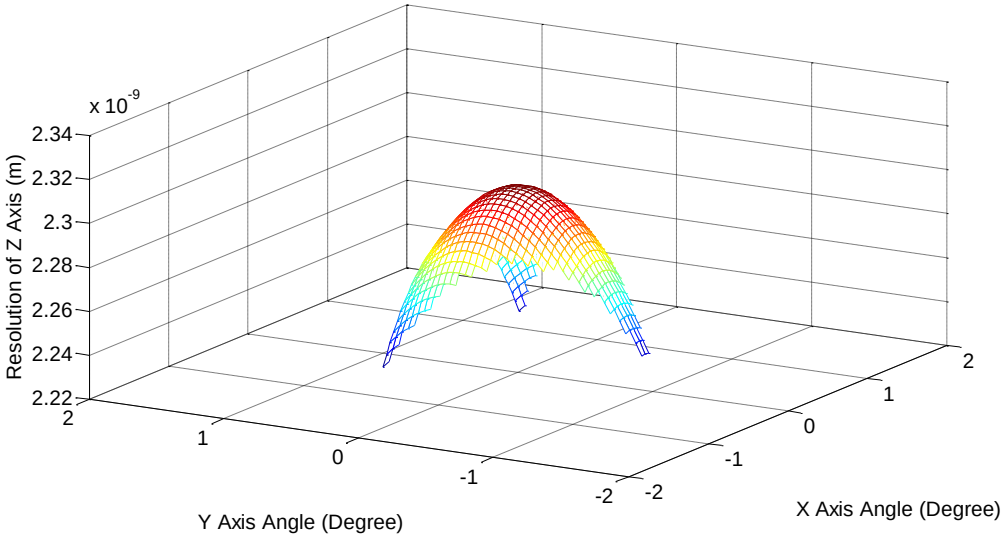

(a) Z=100um plane's resolution distribution

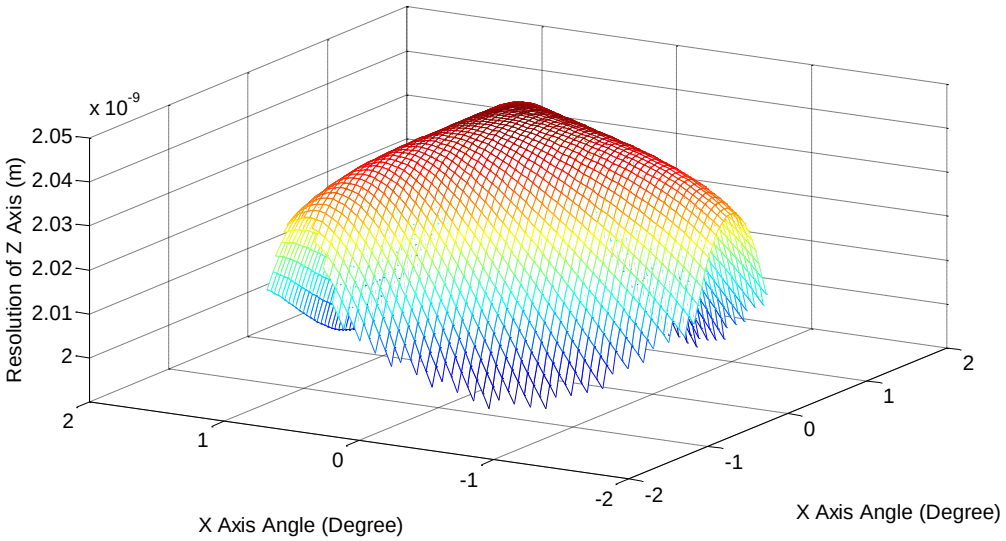

(b) Z=220um plane's resolution distribution

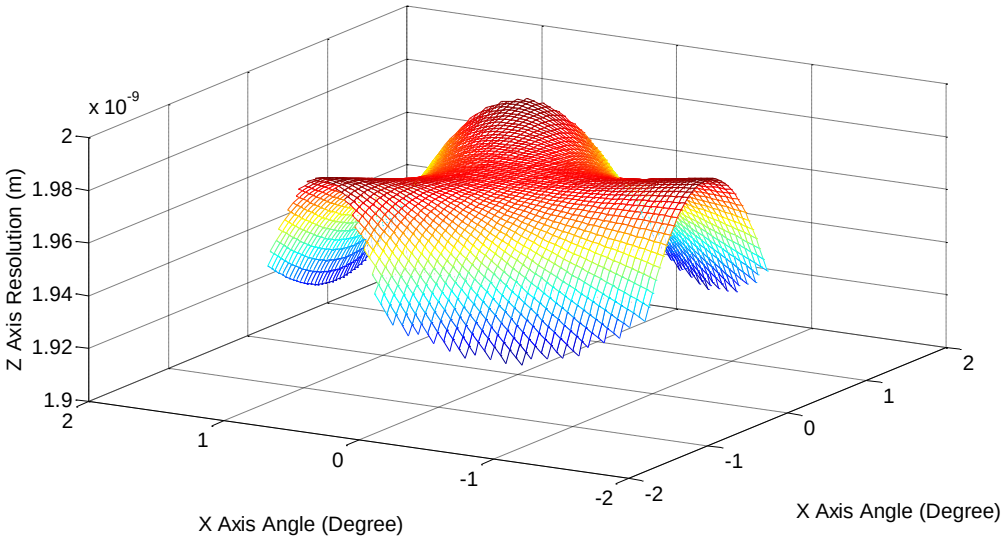

(c) Z=250um plane's resolution distribution

Figure 7. The resolution distribution of the proposed parallel micro manipulator

5. Conclusion

This paper deals with the robotics analysis of a novel 3-DOF parallel micro-robot based on micro gas bubbles actuator. The kinematics model of the proposed parallel micro-robot has been established in which both the geometrical constraint and the force constraint are considered. The performance evaluation index, the motion capability and resolution performance of the parallel micro manipulator has been both analyzed based on the kinematics model, which shows that the proposed parallel micro manipulator is a promising candidate with micro level motion range and nanometer level resolution. The proposed system indicates the feasibility of the micro gas bubbles' application in multiple DOFs parallel micro manipulators, which can be can be extended to a variety of applications in micro domain.

References

[1] Ivan A, Rakotondrabe M, Lutz P and Chaillet N 2009 Current integration force and displacement self-sensing method for cantilevered piezoelectric actuators *Rev Sci Instrum* **80** 126103

[2] Ouyang P R, Tjiptoprodjo R C, Zhang W J and Yang G S 2008 Micro-motion devices technology: the state of arts review *Int J Adv Manuf Tech* **38** 463-78

[3] Xie J, Mane X P, Green C W, Mossi K M and Leang K K 2010 Performance of thin piezoelectric materials for pyroelectric energy harvesting *J Intell Mater Syst Struct* **21** 243-9

[4] Auernhammer D, Kohl M, Krevet B and Ohtsuka M 2009 Intrinsic position sensing of a Ni-Mn-Ga microactuator *Smart Matel Struct* **18** 104016

[5] Bellouard Y 2008 Shape memory alloys for microsystems: a review from a material research perspective *Mater Sci Eng A* **481-482** 582-9

[6] Nespoli A, Besseghini S, Pittaccio S, Villa E and Viscuso S 2010 The high potential of shape memory alloys in developing miniature mechanical devices: A review on shape memory alloy mini-actuators *SensorActuat A* **158** 149-60

[7] Greef A D, Lambert P and Delchambre A 2009 Towards flexible medical instruments: review of flexible fluidic actuators *Precis Eng* **33** 311-21.

[8] Daerden F and Lefeber D 2002 Pneumatic artificial muscles: actuators for robotics and automation *Eur J Mech Env Eng* **47** 10-21

[9] Konishi S, Kawai F and Cusin P 2001 Thin flexible end-effector using pneumatic balloon actuator *Sensor Actuat A* **89** 28-35

[10] Lenders C, Gauthier M and Lambert P 2009 Microbubble generation using a syringe pump *IEEE/RSJ Conf IROS2009* 1395-400

[11] Lenders C, Gauthier M and Lambert P 2011 Parallel microrobot actuated by capillary *IEEE Conf ICRA2011* 6015-20

[12] Lenders C, Gauthier M, Cojan R and Lambert P 2012 Microrobotic platform based on capillary actuation *IEEE T Robot* accepted

[13] Ng C C, Ong S K and Nee A Y C 2006 Design and development of 3-DOF modular micro parallel kinematic manipulator *Int J Adv Manuf Tech* **31** 188-200

[14] Elwaleed A K, Nik A M, Mohd J M N and Mohd M M 2008 A new method for actuating parallel manipulators *SensorActuat A* **147** 593-9

[15] Yue Y, Gao F, Zhao X and Ge Q 2010 Relationship among input-force, payload, Stiffness and displacement of a 3-DOF perpendicular parallel micro-manipulator *Mech Mach Theory* **45** 756-71

[16] Yao Q, Dong J and Ferreira P M 2007 Design, analysis, fabrication and testing of a parallel-kinematic micropositioning *XY* stage *Int J Mach Tool Manu* **47** 946-61

[17] Morita T, Yoshida R, Okamoto Y and Higuchi T 2002 Three DOF parallel link mechanism utilizing smooth impact drive mechanism *Precis Eng* **26** 289-95

[18] Varadarajan K M and Culpepper M L 2007 A dual-purpose positioner-fixture for precision six-axis positioning and precision fixturing Part I. Modeling and design *Precis Eng* **31** 276-86

[19] Mukhopadhyay D, Dong J, Pengwang E and Ferreira P 2008 A SOI-MEMS-based 3-DOF planar parallel-kinematics nanopositioning stage *SensorActuat A* **147** 340-51

[20] Brouwer D M, Jong B R, Boer M J, Jansen H V, Dijk J, Krijnen G J M and Soemers H M J R 2009 MEMS-based clamp with a passive hold function for precision position retaining of micro manipulators *J Micromech Microeng* **19** 065027

[21] Brouwer D M, Jong B R and Soemers H M J R 2010 Design and modeling of a six DOFs MEMS-based precision manipulator *Precis Eng* **34** 307-19

[22] Seo T W, Kim H S, Kang D S and Kim J 2008 Gain-scheduled robust control of a novel 3-DOF micro parallel positioning platform via a dual stage servo system *Mechatronics* **18** 495-505

[23] Kang D S, Seo T W, Yoon Y H, Shin B S, Liu X J and Kim J 2006 A micro-positioning parallel mechanism platform with 100-degree tilting capability *CIRP Ann-Manuf Techn* **55** 377-80

[24] Dong W, Sun L N and Du Z J 2007 Design of a precision compliant parallel positioner driven by dual piezoelectric actuators *SensorActuat A* **135** 250-6

[25] Won J M, Lee J H, Lee K H, Rhee K and Chung S K 2011 Propulsioin of water-floating objects by acoustically oscillating microbubbles *Int J Precis Eng Man* **12** 577-80

[26] Chung S K and Cho S K 2008 On-chip manipulation of objects using mobile oscillating bubbles *J Micromech Microeng* **18** 125024

[27] Marnottant P and Hilgenfeldt S 2004 A bubble-driven microfluidic transport element for bioengineering *Proc Natl Acad Sci* **101** 9523-7

[28] Kwon J O, Yang J S, Lee S J, Rhee K and Chung S K 2011 Electromagnetically actuated micromanipulator using an acoustically oscillating bubble *J Micromech Microeng* **21** 115023

[29] Ho C T, Lin R Z, Chang H Y and Liu C H 2005 Micromachined electrochemical t-switches for cell sorting applications *Lab Chip* **5** 1248-58

[30] Maxwell R B, Gerhardt A L, Toner M, Gray M L and Schmidt M A 2003 A microbubble-powered bioparticle actuator *J Microelectromech Sys* **12** 630-40

[31] Hu W, Ishii K S and Ohta A T 2011 Micro-assembly using optically controlled bubble microrobots *Appl Phys Lett* **99** 094103

[32] Kao J, Wang X, Warren J, Xu J and Attinger D 2007 A bubble-powered micro-rotor: conception, manufacturing, assembly and characterization *J Micromech Microeng* **17** 2454-60

[33] Chung S K and Cho S K 2009 3-D manipulation of millimeter- and micro-sized objects using an acoustically excited oscillating bubble *Microfluid Nanofluid* **6** 261-5

[34] Lambert P 2007 Capillary Forces in Microassembly: Modeling, Simulation, Experiments and Case Study. Microtechnology and MEMS Springer